Reactivity kinetics of sol-gel derived 52S4 glass versus the treatment temperature

Fatima-Zohra Mezahi, Anita Lucas-Girot, Hassane Oudadesse, Abdelhamid Harabi

Reactivity kinetics of sol-gel derived 52S4 glass versus the treatment temperature

Fatima-Zohra Mezahi [a,b], Anita Lucas- Girot[c], Hassane Oudadesse[c], Abdelhamid Harabi[b]

[a] Physics department. M[ed] Boudiaf University. M'Sila. Algeria

[b] Ceramics Lab. Physics Department. Constantine Mentouri University. Constantine. Algeria

[c] Université de Rennes 1. Institut des Sciences Chimiques de Rennes. UMR-CNRS 6226. Rennes. France

Corresponding author: Fatima-Zohra Mezahi; mezahif@yahoo.fr; Ceramics Lab. Physics department, Constantine Mentouri University, Constantine, +213 31 81 11 26; Fax: +213 31 81 11 26.

Abstract

This work is devoted to study the reactivity of the quaternary glass 52S4 (52 % SiO_2 -30 % CaO - Na_2O - 14% 4 % P_2O_5 (wt. %)), synthesized by sol-gel process, versus the treatment temperature. The dried gel was heat-treated at 600 and 650 °C and soaked in Simulated Body Fluid (SBF). XRD results confirm the amorphous character of glass treated at 600 °C even though the heat treatment at 650 °C induces $Na_2Ca_2Si_3O_9$ formation. After soaking in SBF, SEM and EDS results show the formation of carbonated hydroxyapatite (HA) at the glass surface for both temperatures. For the glasses treated at 600 and 650 °C, two phenomena were observed: the glass dissolution in SBF and the carbonated HA precipitation but the reactivity kinetics of glass was different when temperature changes. For SGDG600, the carbonated HA began to crystallize after 16 h and became well crystallized after 15 days. For SGDG650, a glass ceramic made of a glassy matrix and of $Na_2Ca_2Si_3O_9$, the crystallized carbonated HA was observed after 2 h. In addition a new crystallization at the glass surface of $Na_2Ca_2Si_3O_9$ was observed after 15 days.

Keywords

Sol-Gel process; Temperature; Simulated Body Fluid; Kinetics reactivity; Bone like- apatite.

1. Introduction

Bone defect filling or reconstruction required a wide research and development of biocompatible and bioactive materials. The bioactive material, in contact with physiological solutions, elicits a specific biological response at the interface of the material which results in the formation of a direct biochemical link (carbonated hydroxyapatite) when it is implanted in human body [1]. Since Hench has launched the concept of bioactive glass, many new materials and products have been prepared from variations on bioactive glasses [2], glass–ceramics [3] and ceramics such as synthetic and natural hydroxyapatite (HA) [4-13], wollastonite [14-16] and diopside [17,18]. Hench *et al.* have demonstrated that glass with the molar composition: 46.1 % SiO_2, 24.4 Na_2O, 26.9 CaO and 2.6 % P_2O_5, termed Bioglass® 45S5, is able to develop, at the interface with body fluids, an apatite like layer similar to bone mineral. This bond is so strong that it could not be removed without breaking the bone [1]. However, the poor mechanical strength and toughness of bioactive glass have restricted their use in several clinical applications. To resolve this problem and consequently to broad the range of clinical applications, the glasses were transformed into glass–ceramics [19-21]. Despite these benefits, contradictory results were published on the reactivity and biological interest of these glass ceramics (crystalline or semi-crystalline). They may be less soluble in body fluid and the mineral formation rate and bone integration at the tissue-material interface may be affected [22-24]. At the same time, the crystallization of some glassy systems significantly decreases their bioactivity in comparison with the same amorphous glassy systems [19-21]. Li *et al.* [25] showed that a bioactive glass can be transformed into an inert glass-ceramic. *In vitro* test showed that the carbonated HA layer was formed only if the glass ceramic contain over 90% of a residual glassy phase. Whereas, Peitl *et al.* [23,24] have developed the first bioactive glass–ceramic in the SiO_2–CaO–Na_2O–P_2O_5 system with both good mechanical properties and high bioactivity. It contains about 30 to 65% crystalline phase, and the main phase is $Na_2Ca_2Si_3O_9$. After that, Ravagnani *et al.* developed a highly bioactive fully crystalline glass–ceramic in SiO_2–CaO–Na_2O–P_2O_5 system (Biosilicate® glass–ceramic) [26]. Almost all the works have shown that $Na_2Ca_2Si_3O_9$ formation, observed in some glass-ceramics, enhances the mechanical properties of the starting glass and maintains the high bioactivity of particular compositions in the SiO_2–CaO–Na_2O–P_2O_5 system. Peitl *et al.* have shown that glass crystallisation decreased development kinetics of a carbonated HA layer but did not inhibit its formation, even in fully crystallized ceramics [24]. In 2011, Siqueira *et al.* have shown that $Na_2Ca_2Si_3O_9$, formed in SiO_2–CaO–Na_2O–P_2O_5 system, has bioactivity behaviour similar to that of Biosilicate® glass–ceramic [27].

In the our previous works, a glass with the new composition (wt%) 52% SiO_2- 30% CaO- 14% Na_2O- 4% P_2O_5 (mol%: 52.3% SiO_2- 32.3%CaO- 13.7%Na_2O- 1.7% P_2O_5) (named 52S4) was synthesized both by melting and an original sol- gel route [28]. The effect of synthesis mode on glass bioactivity after soaking in simulated body fluid (SBF) was investigated [29]. The dried gel was then heat treated at 550°C (below the crystallization temperature). The obtained results showed that the main differences between the Sol-Gel Derived Glass (SGDG) and Melting Derived Glass (MDG), from the structural and textural point of view, are induced by the synthesis mode. The obtained results have led to conclude that 52S4 is a bioactive glass if it is prepared by the two routes: melt and sol-gel. However, this glass was more reactive when it was prepared by sol-gel method. The sol-gel route enhanced fast and continuous glass resorption associated to the early formation of the bone like-apatite at the glass surface. However, the HA did not crystallized even after 30 days. This result was attributed to a continuous formation of silica gel up to the amorphous apatite layer.

The aim of the present study is to investigate a possible evolution in reactivity behaviour of the sol-gel derived glass by increasing the thermal treatment temperature previously used [28,29].

2. Experimental section

2.1. Material preparation

The sol-gel process was used to prepare the following glass composition 52S4: (wt.%) 52% SiO_2- 30% CaO- 14% Na_2O- 4% P_2O_5. The glass synthesis was described in detail previously [28]. The glass was prepared in a hermetically cylindrical Teflon container from high-purity raw materials as tetraethyl orthosilicate TEOS: Si $(OC_2H_5)_4$ (>98%, Fluka), triethylphosphate TEP: OP $(C_2H_5)_3$ (>99.8 %, Sigma-Aldrich), calcium carbonate $CaCO_3$ (>98.5%, Merck) and sodium carbonate Na_2CO_3 (>99.5%, Merck). Accurately weighed amounts of these reactants were added, one by one each hour under magnetic stirring, to a 2 M aqueous acetic acidic solution. The resultant sol was kept for hydrolysis and polycondensation at room temperature for 6 days. After that, it was kept at 70°C for 3 days and dried at 150°C for 52 h.

In this study, 52S4 glass is studied in two different microstructural forms (amorphous and partially crystalline). The obtained dried-gel was thermally treated at 600 and 650°C (noted SGDG600 and SGDG650) during 3 h under vacuum with a heating rate of 0.5°C.min^{-1}. Let's remember that the domain of thermal stabilization of the dried gel is between the transition temperature T_G (T_G=

596°C) and the crystallization temperature T_C (T_C= 631°C) as determined by Thermo-Gravimetric associated with Differential Scanning Calorimetry (TG/DSC) analyses [28].

2.2. In vitro assays

To evaluate the kinetic reactivity of the prepared glasses, SBF (SBF-K9 type) was used as soaking solution which has the ion concentrations similar to those in human blood plasma. According to Kokubo's protocol [30], the SBF was prepared by dissolving reagent-grade $CaCl_2$, NaCl, KCl, $MgCl_2.6H_2O$, $K_2HPO_4.3H_2O$ and $NaHCO_3$ in distilled water. It was buffered at pH 7.4 with (hydroxymethyl)-aminomethane [$(CH_2OH)_3CNH_2$] and hydrochloric acid (HCl). The glasses were soaked in SBF in the form of disks. 0.5 g of the dried gel in powder, with particle sizes ranged from 40 to 63 μm, were compacted at 675 MPa under cold uniaxial pressing. After that, the compacted dried gel disks were heat treated under the conditions mentioned before. The ratio between the geometric areas of disks and the volumes of SBF was adjusted to 0.075 cm^{-1}. The glasses were kept in SBF at 37°C for time periods ranging from 2 h to 30 days (SBF immersion tests were carried out in triplicate). After soaking, the disks were emerged from SBF, washed with ethanol and dried in air.

2.3. Materials Characterization

Different techniques and apparatus were used to study the physical and chemical properties of prepared glasses before and after soaking in SBF.

The specific surface area and porosity measurements were performed using multi-point BET, ASAP 2010 Micromeritics). In addition, the phase compositions were identified using X-ray diffraction (XRD) data collected in a BRUKER, D8 ADVANCE with a CuKα radiation (λ = 0.154 nm, filter: Ni, voltage= 30 kV and current= 20 mA, step = 0.05°, scan step time= 10 s). To improve the structural analysis, Fourier Transformed Infra-Red spectroscopy (FTIR) (BRUKER EQUINOX 55) was used. 1 mg of material scraped from the glass surface was mixed with dried KBr to perform the FTIR studies. The microstructure of glass surfaces was observed using a Scanning Electron Microscope (SEM) (HITACHI, JSM-6301 F) working at a 7 kV as an accelerating voltage. Before observation and EDS analyses (Oxford Link INCA), the surfaces were gold- coated (Au- 20 wt% Pd) in order to allow surface conduction. For the *in vitro* tests in SBF, Inductively Coupled Plasma-Optical Emission Spectroscopy (ICP-OES) (SPECTRO Ciros Vision) technique was used to evaluate the variations of silicon, calcium and phosphorous concentrations versus soaking time in SBF.

3. Results

3.1. Characteristics of 52S4SGDG before soaking in SBF

3.1.1. Specific surface area and porosity

The BET specific surface area and pore volume of SGDG decreased when temperature increased from 600 to 650°C. Their values are in order: 18.26 $m^2.g^{-1}$ and 0.058 $cm^3.g^{-1}$ (for SGDG600) and 6.00 $m^2.g^{-1}$ and 0.013 $cm^3.g^{-1}$ (for SGDG650), respectively. Also, the median pore diameter decreased from 127 Å (for SGDG600) to 88.34 Å (for SGDG650).

3.1.2. X- ray diffraction

Figure 1 shows the XRD data for SGDG600 and SGDG650. The XRD of SGDG600 showed that the final product is mainly amorphous. However, the data reveal that the glass exhibited a very low crystallization of hydroxyapatite (HA) before any immersion in SBF, as for the glass treated at 550°C [28]. In addition, two diffusion halos are observed in the range 27°-34° and 15°-23° (2θ). Analogous maxima were obtained by Martinez *et al*. in their study of binary glasses SiO_2-CaO. They attributed the diffraction maximum between 28 and 34° 2θ to the incipient presence of different crystalline phases of calcium silicates, whereas the maximum at 22.5°2θ to a formation of SiO_2 content in the glass [31]. Otherwise, DRX of SGDG650 confirmed the $Na_2Ca_2Si_3O_9$ crystallization (ICDD powder diffraction: file n° 22.1455), in a glassy matrix. The HA phase is also present as a very minor phase.

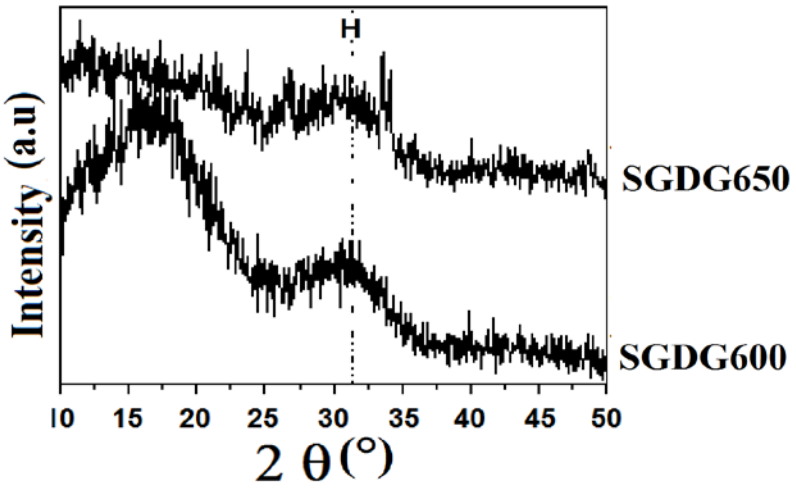

Fig. 1. X-ray diffraction patterns of SGDG heated at 600°C and 650°C.

H: HA

3.1.3. Infrared studies

Figure 2 shows the FTIR spectra of all glasses. They exhibit the same IR bands. As discussed in early work [28], the observed bands at 500, 762 and 1035 cm^{-1} are assigned to silicate network vibrations Si-O-Si. The band observed at 606 cm^{-1} is related to P-O bending in crystalline HA [32,33]. This band was reinforced with temperature mainly at 650°C, which confirms the crystallisation of HA during heat treatment. In the other hand, the band located at 500 cm^{-1} become more intense when the temperature increases. This band may be attributed to the crystal phase $Na_2Ca_2Si_3O_9$ [24,34]. The bands at 933 and 762 cm^{-1}, related to Si-O-Si stretching of non-bridging oxygen atoms [33], are better defined in all spectra. The bands at 870, 1419 and 1496 cm^{-1} are related to the presence of CO_3^{2-} groups [35]. The intensity of these bands is weak.

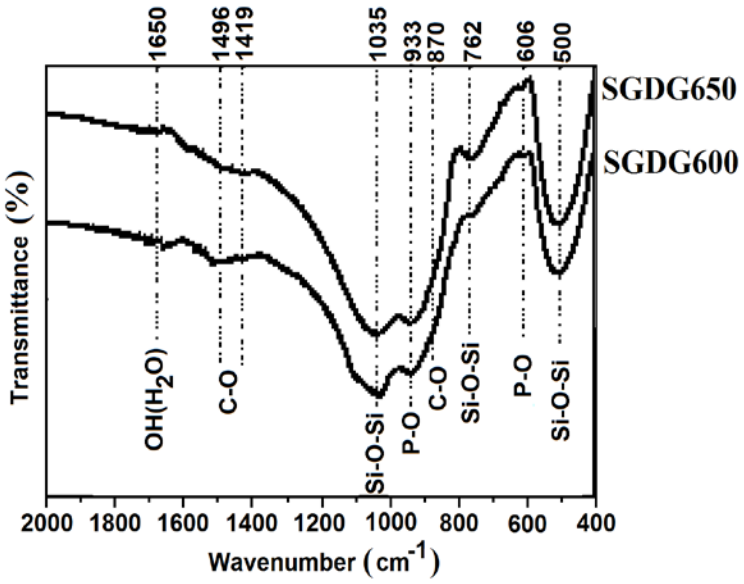

Fig. 2. FTIR spectra of SGDG heated at 600°C and 650°C.

3.2. In vitro assays results

In order to evaluate the formation kinetics of bone like apatite at surface of soaking glass in SBF, the pH and variations in Si, Ca and P concentrations in SBF were measured. The study was accomplished by analyzing the formed apatite layer at the glasses surface by XRD, FTIR and SEM-EDS techniques.

3.2.1. ICP results and pH measurements

Figure 3 presents ICP results and pH measurements.

The Ca concentration evolution followed a similar tendency for the two materials (Fig.3-a). For the both materials, it decreased slowly at the first soaking hours. After that, for SGDG600, this concentration increased slowly until 1 day where it increased dramatically and reached a maximum value. The maximum calcium release from glass surface is achieved after 7 days. After that a continuous decrease in Ca concentration was observed up to 30 days. For SGDG650, the maximum value for the Ca concentration in SBF was reached after 3 days, then decreased strongly and remained constant in the interval time 7- 30 days.

During the experiment, P concentrations in SBF decreased continually (Fig. 3- b) for the both materials. This indicates that the amount of P released from glass or glass-ceramic surfaces did not compensate its consumption due to the apatite formation. It can be observed that P concentrations were nil in SBF where SGDG600 was soaked after 7 days and after 15 days for SGDG650. All P ions were consumed from SBF.

The increase in Ca concentration in SBF is a result of Ca ions leaching from SGDG surface to SBF. However, the decrease in the Ca and P concentrations in SBF is attributed to the rapid growth of the apatite at the glass surface that overcame the release rate of Ca and P ions to SBF [31].

As SBF is initially silicon –free, the presence of Si in SBF is consistent with a release of this element from the glass surface to the soaking solution. The Si concentration in SBF increased with soaking time for both materials (Fig.3-c). The Si concentration increased strongly in the first hours for SGDG600 and SGDG650. However, there was a fluctuation in Si concentration during soaking time from 16 h to 15 days for SGDG600. For SGDG650, the increase in Si concentration was continuous.

The pH evolution is relevant to the dissolution process of glasses soaked in physiological solutions. The increase in pH of SBF is the result of ion exchanges between the protons H^+ in SBF and the glass modifying cations. The pH value of SBF increased strongly after 2 h soaking time for both glasses (Fig.3-d). For SGDG600, the pH was stable around 8.3 between 4 h and 1 day. The increase in pH values was not continuous: a fluctuation occurred in the interval 3-15 days. Between 3 and 7 days, the increase in pH value was followed by a slight decrease between 7 and 15 days. A more noticeable increase in pH value occurred after 30 days. It achieved 9.9 units. For SGDG650, pH evolution follows the same trend than that of SGDG600. However, the fluctuation in pH values occurred in the 1- 7 days interval. After that, an important increase occurred in pH value which achieved 10 units after 30 days. In general, the pH values for SGDG650 were lower than that of SGDG600.

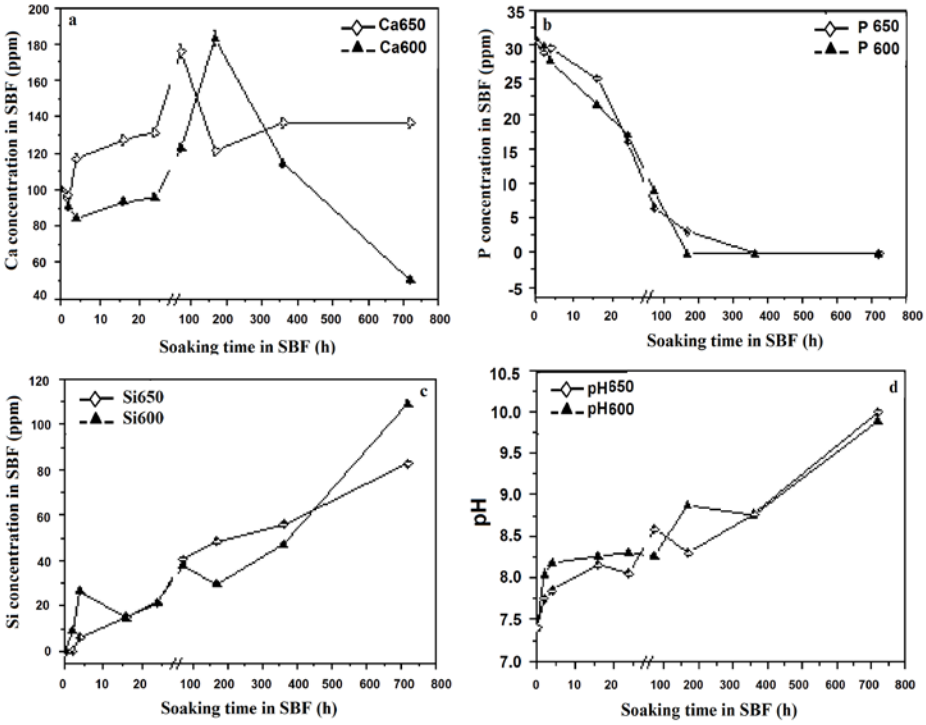

Fig. 3. Evolutions of Ca (a), P (b) and Si (c) concentrations in SBF, and evolution of SBF pH (d), versus soaking time of SGDG heated at 600°C and 650°C.

3.2.2. Structural modifications after soaking in SBF

3.2.2.1. XRD results

According to XRD data for SGDG600 surface, after soaking in SBF (Fig.4), crystalline HA peaks appeared only after 15 days (natural HA, prepared from calcined bovine bone, was used as a reference [7]). Before this time, it is difficult to distinguish this phase. Noted that after 7 days, the XRD data revealed the formation of calcite, justified by the apparition of its most intense peak at 29.4° (2θ) (ICDD powder diffraction: file n^{o} 86.2334). The intensity of this peak increased with time and it became a major visible phase on XRD diagram after 30 days. As a consequence, the intensity of crystallized HA peaks decreased between 15 and 30 days.

For SGDG650, the crystalline HA peaks appeared on the XRD pattern after 2 h. The peaks intensity of HA increased after 4 h. Additionally, XRD highlighted the presence of $Na_2Ca_2Si_3O_9$ phase at the same time. This latter phase became the dominant crystallized phase after 16 h, as the peaks intensity of HA became lower. Between 4 h and 1 day, XRD also revealed the presence of an amorphous phase at the glass-ceramic surface. A broad halo was appeared around 20°C which can

be attributed to silica gel [36]. After that, the peaks intensity of HA increased and those of $Na_2Ca_2Si_3O_9$ decreased up to 7 days when the peaks intensity of the two phases were similar. After 15 days, $Na_2Ca_2Si_3O_9$ appeared again as the mainly formed phase. After 30 days, the calcite peak was present. Consequently, it can be observed that the peaks intensities of previous existent phases HA and $Na_2Ca_2Si_3O_9$ decreased strongly.

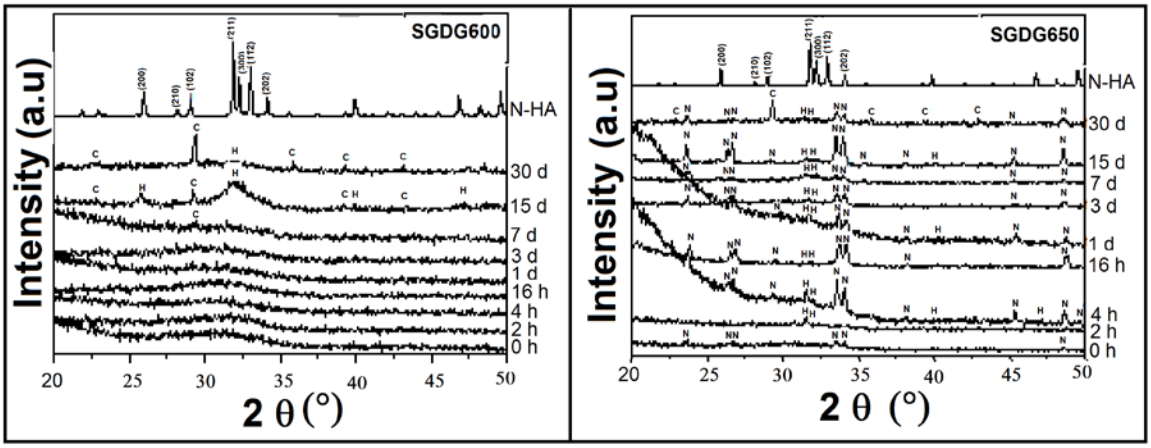

Fig. 4. XRD patterns of SGDG600 and SGDG650 surfaces before and after soaking in SBF solution at different testing times.

H: HA, C: $CaCO_3$, N: $Na_2Ca_2Si_3O_9$.

3.2.2.2. FTIR results

In SGDG600 spectra (Fig.5-a), between 2 and 4 h, the characteristic peaks of amorphous HA appeared at 464 cm^{-1} and a broadening band situated around 1056 cm^{-1} [33]. The presence of crystallized HA was confirmed after 16 h by the apparition of a weak new peak at 560 cm^{-1} and reinforcement of band situated at 605 cm^{-1}. These bands are distinguishable until 15 days. Additionally, the characteristic bands of C-O vibrations, mainly attributable to calcite, appeared after 7 days and are clearly visible after 15 days. Also, these bands can be attributed to C-O in carbonated HA. As indicated by XRD, after 30 days, the calcite was present simultaneously with crystallized HA. In IR spectra, the characteristic bands of glass network progressively disappeared with time which led to conclude that carbonated HA layer is dense.

A new weak band at 823 cm^{-1}, characteristic of Si-O symmetric stretching vibrations [33,37], appeared after 1 day. This band was also present until 15 days. This result confirms the formation of a Si-rich layer at the glass surface.

For SGDG650 (Fig.5-b), no difference appeared between spectra before soaking and after 2 h in SBF. After 4 h, the characteristic bands of P-O appeared at 454, 533 cm^{-1} and a weak band at about 610 cm^{-1}. These bands confirmed the formation of crystallized HA. These bands were reinforced until 3 days. After 7 days, the intensity of the band situated at 533 cm^{-1} decreased and another band, characteristic of P-O vibration in crystallised HA, appeared at 562 cm^{-1}. No change occurred after 15 days. After 30 days, the band situated at 533 cm^{-1} merged in the band situated at 562 cm^{-1}. In addition, the intensity of the band situated at 610 cm^{-1} decreased. It can be observed that the intensity of band at 933 cm^{-1}, related to Si-O-Si vibration, decreased with soaking time. Also, the band around 1040 cm^{-1} becomes sharp and two other bands characteristic of P-O in HA appeared at 1045 and 1085 cm^{-1}. The characteristic bands of C-O situated at 870, 1420 and 1496 cm^{-1} were clearly visible after 3 days which led to conclude that the formed apatite is carbonated HA. These bands were also well noticeable after 30 days. According to XRD results, these bands are attributable to $CaCO_3$ phase and carbonated HA. A weak band appeared at 800 cm^{-1} [33,37], which is characteristic band of Si-O symmetric stretching vibrations, after 4 h and 1 day. This band reappeared strongly after 7 day.

Hence, the FTIR results are in a good agreement with XRD results.

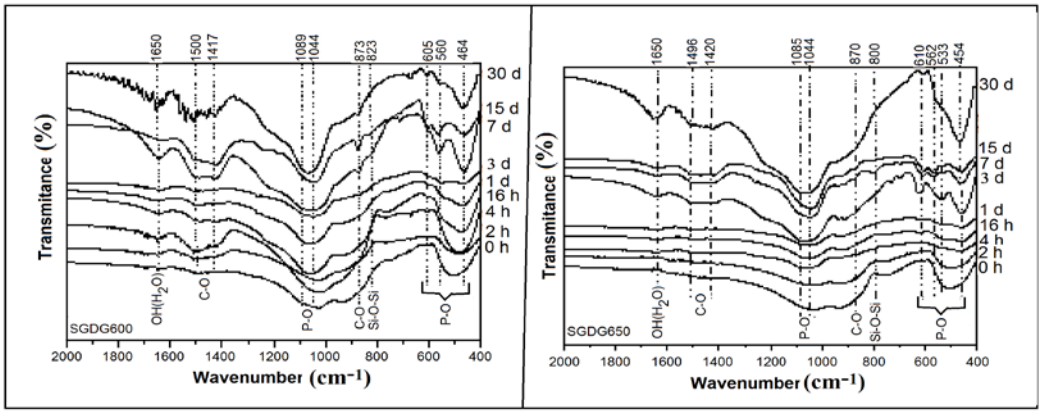

Fig. 5. FTIR spectra of SGDG600 and SGDG650 before and after soaking in SBF.

3.2.2.3. SEM-EDS results

SEM images and EDS analyses (Fig.6) depicted the morphological modifications and composition evolutions of SGDG600 surface with soaking time. After 2 h, a new layer, formed by spherical particles, dispersed at the glass surface. The EDS analysis, with the significant increase in phosphorous concentration, confirmed the formation of an apatite layer at the glass surface after 2h in SBF as suggested by FTIR and ICP results. This layer becomes denser with time. However, after 30 days, the Ca and P concentrations decreased. According to ICP result, the P concentration was nil between 7 and 30 days. So, there were not P ions to lead to continuous apatite formation. In addition, SBF is saturated by carbonate ions which led to calcite formation up to crystallized carbonated HA (The characteristic rhombohedral particles of $CaCO_3$ as calcite were not observed at the glass surface giving evidence of the presence of this phase as localized precipitate and not as surface controlled phase).

The Si concentration decreased at the glass surface after 15 days. This result is consistent with the formation of a dense apatite layer at the glass surface. However, the Si concentration increased after 30 days. This result may be related to the presence of Si in the apatite layer due to the continuous Si release between 7 and 30 days revealed by ICP analyses or to a new visibility of the silica gel formed at 7 days (as evidenced by IR analysis) due to the impossibility of the apatite layer formation to progress without phosphorous ions in SBF.

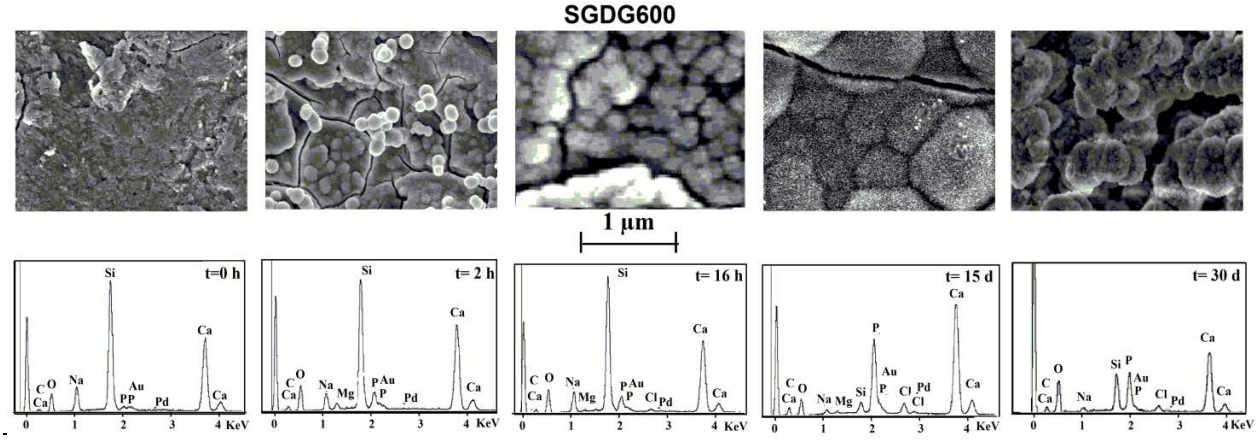

Fig. 6. SEM micrographs and EDS spectra of SGDG600 surfaces before and after soaking in SBF.

The morphological modifications of SGDG650 surface with soaking time were depicted by SEM images and EDS analyses (Fig.7). After 2 h, some spherical particles dispersed on a uniform gel formed at the glass surface. The EDS analysis showed that there was a slight increase in both Si and P at the glass surface. This layer is attributed to silica gel and the spherical particles to apatite layer

as it was confirmed by XRD and ICP results. After 4 h, the SEM images showed that there were two phases one up to another with different morphologies. The EDS analyses showed a significant increase in P concentration at the glass surface. This result, associated to the ICP analyses ones, is consistent with the formation of the apatite layer the glass surface up to the silica gel layer. After 1 day, this phase becomes compact as confirmed by EDS analysis. After 3 days, it is very difficult to distinguish the grain boundaries. A formed gel has covered the totality of the last layer. The IR analysis showed the formation of silica gel justified by apparition of Si-O-Si band at 800 cm^{-1}. After 7 days, a very dense layer was formed. The entire glass surface was covered with compacted needle-like crystallites, very rich in Ca and P elements, consistent with aggregates of carbonated HA. In addition, the ICP results showed that Ca and P ion concentrations decreased mainly in SBF after 7 days. After 15 days, another phase was formed up to the carbonated HA layer. The EDS analyses showed that one phase was rich in Ca and P ions and poor in Si and Na. The other phase was rich by Si, Na and Ca and poor in P. According to XRD diagram, the two phases are HA and $Na_2Ca_2Si_3O_9$. Finally, after 30 days, a new layer was formed at the glass surface. This layer of crystallized HA had a different morphology than that at 15 days.

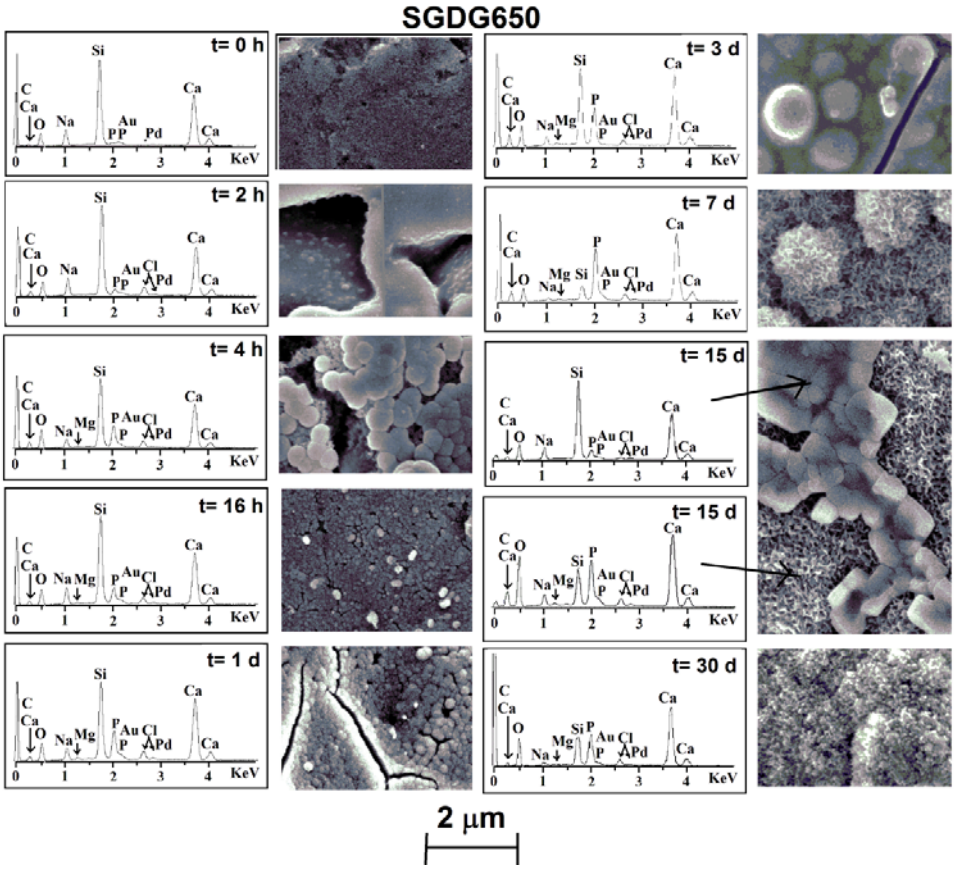

Fig. 7. SEM micrographs and EDS spectra of SGDG650 surfaces before and after soaking in SBF.

4. Discussion

The heat treatment at 650°C, above the temperature of crystallization outset [28], induced the crystallization of $Na_2Ca_2Si_3O_9$ in a mainly amorphous matrix. Compared with the two others materials SGDG550 [29] and SGDG600, SGDG650 is a glass-ceramic.

Results indicate that each material, synthesized with a same initial composition 52S4SGDG exhibited, after a different heat treatment, special reactivity features.

The bioactivity characteristic is associated to the occurrence of successive steps. As described by Hench for bioactive glasses [38] and Kokubo [39] for bioactive materials containing $CaO\text{-}SiO_2$, a hydrated silica layer is formed at the surface prior to the deposition of HA. After rapid exchange of glass modifier cations (Na^+ and /or Ca^{2+}) with H^+ in solution, the soluble silica is loosed as $Si(OH)_4$ by breaking of Si-O-Si bridges and subsequent silanol Si-OH groups are formed at the material surface. After that, silanol groups condense and their polymerization forms a SiO_2 rich surface layer. Silica gel thickness increases with glass surface leaching [40]. Up to this layer, $CaO - P_2O_5$ rich layer forms and further crystallized as carbonated HA layer [38,41-43]. The nuclei thus-formed later grow at the expense of the ions in the solution that was saturated with respect to apatite. Kim *et al*. [44] reported that glasses with <50 mol% SiO_2 form a Ca–P-rich layer and a Si layer simultaneously while glasses with >50 mol% SiO_2 form a Ca–P layer on the top of a Si-rich layer. These differences are related to the glass structure in relation with composition.

Dissolution rates and SiO_2 rich layer formation are mainly associated to the evolution of silicon concentration and pH of SBF. Also, the formation of carbonated HA layer is associated to the evolution of calcium and phosphorous concentrations in SBF. These results indicate that the three different materials: SGDG550, SGDG600 and SGDG650 presented different features.

By comparing to the previous ICP results [29], SGDG600 have similar behavior than SGDG550 up to 4 h soaking: an important release of silicon and an increase of pH above 8. During this time, calcium and phosphorous concentrations decrease in SBF for the two glasses. As confirmed by ICP, RX, IR and EDS results, the formation of carbonated HA layer occurred simultaneously to the glasses dissolution. Our results are in accordance with those of Kim *et al*. [44] who reported that glasses with 50 mol % SiO_2 form a Ca–P-rich layer and a Si layer simultaneously. Our glass contains 52.3% SiO_2 close to 50% mol.

In our previous work for SGDG550 [29], Si concentration in SBF increased up to 3 days before a decrease which was consistent with the formation of the SiO_2 layer. The successive silica layers were formed during soaking time simultaneously with carbonated HA layers. XRD and FTIR analyses showed that no crystallized apatite phase was formed at the SGDG550 surface even after

30 days. But, after 2 h, the calcite was formed at the glass surface. This phase was previously observed for a glass with a molar composition 60%SiO_2 – 35%CaO – 5% P_2O_5 [45]. The presence of this phase is not related to the glass composition but due to the high concentration of HCO_3^- in SBF that induced, in the presence of high calcium concentrations near the glass surface, the calcite $CaCO_3$ precipitation instead of the surface controlled crystallization of carbonated HA.

For SGDG600, after 4 h, a decrease in Si concentration in SBF was observed. This is consistent with the formation of the SiO_2 layer at the material surface after 1 day. This silica layer was already detected until 30 days. Between 4 h and 7 days, the glass dissolution process is the dominant feature compared to the carbonated HA precipitation process. After 7 days, the HA precipitation predominated the dissolution process as indicated by the decrease of Ca and P concentrations in SBF. IR analysis highlighted the presence of a carbonated apatitic phase between 1 and 7 days. This phase was well crystallized after 15 days as confirmed by XRD and IR results.

The secondary precipitation of calcite $CaCO_3$ is observed after 30 days. This phenomenon is amplified by the total consumption of SBF phosphorous ions after 7 days. As consequence, there were no P ions to allow the continuous apatite formation.

For SGDG650 during the period 0 - 4 h, the silicon release is slower than the two other materials and the pH stays under 8. The pH value stayed under 8 and slowed down the Si dissolution [46] which inhibited the formation of silanol groups Si-OH at the glass surface and consequently their release as $Si(OH)_4$. These results may be related to a lower reactivity of glass-ceramic due to the significant reduction of porosity for SGDG650 comparatively to the other materials associated to a difference in the reaction mechanism related to the presence of the crystallized phase associated to the glass matrix, which induced an inhomogeneity in the reactivity of the material surface.

During the two first hours the glass-ceramic dissolved weakly and a calcium and phosphorous ions uptake by the material surface occurred. The silica gel layer was detected only by SEM analysis, the thickness of this layer was weak and consequently not detectable by IR analysis. Up to this silica layer, the carbonated HA spherical particles was formed as justified by XRD, IR, MEB-EDS results. However, from 2 h to 7 days, a more complex process set up. An important release of calcium from the material occurred. This release was not associated to a proportional release of silicon in SBF. The material dissolution is associated to the simultaneous formation of a new amorphous phase and the reformation of $Na_2Ca_2Si_3O_9$ at the material surface as shown in XRD diagrams. In parallel, between 4 h and 3 days, the Ca and P concentrations at the glass surface increased as demonstrated by EDS analysis which confirm the formation of carbonated HA layer, its densification and grain size enlargement with time. The IR and XRD analysis confirmed this result, the intensity of P-O bands increased with time and the intensity of characteristic XRD peaks

of $Na_2Ca_2Si_3O_9$ decreased with the continuous formation of carbonated HA layer. This particular behavior may be related to the initial presence of $Na_2Ca_2Si_3O_9$ which had a different dissolution rate from the glass matrix. The consistency between the obtained results shows that the dissolution of $Na_2Ca_2Si_3O_9$ was followed by a reprecipitation of this phase at the glass surface, associated to a rapid formation of the calcium free amorphous silicon rich phase and a consecutive formation of the carbonated HA. After 7 days, the Ca and P concentrations in SBF decrease as those at the glass surface achieved their maximum values which is consistent with the densification of carbonated HA layer and its formation as compacted needle-like crystallites aggregates. After 15 days, all P ions in SBF were consumed, and then after 15 days, there were no P ions available to form HA. Calcium ions concentration increased slightly and stabilized between 7 and 30 days as silicon concentration increased continuously during soaking time. These results indicate that the material dissolution went out. The formation of carbonated HA was stopped by lack of phosphorous in SBF and up to 15 days, the reprecipitation of $Na_2Ca_2Si_3O_9$ is favoured. After 30 days, the calcite $CaCO_3$ was formed, up to $Na_2Ca_2Si_3O_9$, by the combination of calcium ions from glass and HCO_3^- from SBF [45].

The temperature treatment has a marked effect on kinetics of carbonated HA formation at the glass surface. One of the important factors associated to bioactivity is ionic exchanges between material and surrounding medium. Porosity and material specific surface area greatly influence these exchanges. According to our results, when the heat temperature increases, the surface area and the pore volume decrease, then the precipitation process became less dominant that the dissolution process which has observed only for glasses treated at 600 °C and 650°C. According to obtained results, when the temperature increases from 600°C to 650°, the glass density increases and consequently the corresponding time of dissolution onset decreases. In addition, the carbonated HA was formed after 2 h at glass surface for all treatment temperature. However, the corresponding time to carbonated HA crystallization decreases with heat treatment. Moreover, the corresponding time for apparition of characteristic bands of silica gel increases with treatment temperature. It was suggested, for SGDG550, that the continuous formation of silica gel at the glass surface during the soaking time inhibited the HA crystallization. For SGDG600 and SGDG650, the thickness of silica layers was thinner and their formation were limited comparatively to SGDG550, which allowed the HA crystallization.

In this work, a special behaviour was observed for SGDG650: $Na_2Ca_2Si_3O_9$ phase, initially present in the material, was reprecipitated at the material surface during soaking time. It can be suggested that the dissolution of this phase occurred and the diffusion of ions promoted the formation of this phase at the glass surface.

So, the heat treatment and the formation of the crystallized phases such as $Na_2Ca_2Si_3O_9$, maintained the high bioactivity of 52S4 as others particular compositions of the SiO_2–CaO–Na_2O–P_2O_5 system in other works [23,24,27,47-50]. Moreover, the heat treatment at 600°C and 650°C allowed the HA crystallization.

5. Conclusion

The obtained results lead to conclude that the bioactivity of 52S4SGDG glass was not affected by the heat treatment modification. For all temperatures, carbonated HA was formed at the material surface after soaking in SBF. For SGDG550, the carbonated HA remained amorphous even after 30 days and it was formed up to the silica layer which reformed at any time. For SGDG600, carbonated HA began to crystallize after 16 h and became well crystallized after 15 days. However, the heat treatment at this temperature did not prevent the reformation of a silicon oxide layer up to the carbonated HA one. The silica layer was detected later than the carbonated HA formation, accordingly to IR results. Otherwise, for SGDG650, the crystallized carbonated HA was observed after 2 h. In addition, the crystallized phase $Na_2Ca_2Si_3O_9$ in the initial material before soaking was reprecipitated at the glass surface after 15 days.

This study highlighted the original behavior of this new composition and the possible adjustment of reactivity by modifying the heat treatment temperature, without changing the materials bioactive features.

Acknowledgements

The authors would like to thank the authorities responsible for the financial support of this work (M'sila University and Algerian minister of superior education and research). Many thanks to Bernard Lebeuvre (Equipe Chimie du Solide et Matériaux, UMR 6226 Rennes), F. Gouttefangeas (CMEBA centre of UMR-CNRS 6226- Rennes) and D. Laillé (INSA- Rennes) for their fruitful collaborations.

References

[1] Hench L.L., Splinter R.J., Allen W.C. et Greenlee T.K.: Bonding mechanism at the interface of ceramics prosthetic materials. J. Biomed. Mater. Res. Symp. 2, 117-141 (1971).

[2] Hench L.L.: The story of bioglass. J. Mater. Sci: Mater. Med. 17, 967-978 (2006).

[3] Kokubo T.: Bioactive glass ceramics: properties and applications. Biomaterials 12, 155-163 (1991).

[4] LeGeros R.Z.: Properties of osteoconductive biomaterials: Calcium phosphates. Clin. Orthop. Relat. Res. 395, 81-98 (2002).

[5] Mezahi F.Z., Harabi A. et Achour S.: Effect of stabilised ZrO_2 on sintering of hydroxyapatite. Key Eng. Mater. 264-268, 2031-2034 (2004).

[6] Mezahi F.Z., Harabi A., Zouai S., Achour S. et Bernache-Assollant D.: Effect of stabilised ZrO_2, Al_2O_3 and TiO_2 on sintering of hydroxyapatite. Mater. Sci. Forum 492-493, 241-248 (2005).

[7] Mezahi F.Z., Oudadesse H., Harabi A., Lucas-Girot A., Le Gal Y., Chaair H. et Cathelineau G.: Dissolution kinetic and structural behaviour of natural hydroxyapatite vs. thermal treatment : Comparison to synthetic hydroxyapatite. J. Thermal Anal. Calor. 95(1), 21-29 (2009).

[8] Harabi A., Belamri D., Karboua N. et Mezahi F.Z.: Sintering of bioceramics using a modified domestic microwave oven. J. Therm. Anal. Calorim. 104, 283-289 (2011).

[9] Mezahi F.Z., Oudadesse H., Harabi A. et Lucas-Girot A.: Effect of ZrO_2, TiO_2, and Al_2O_3 additions on process and kinetics of bonelike apatite formation on sintered natural hydroxyapatite surfaces. Int. J. Appl. Ceram. Technol. 9, 529-540 (2012).

[10] Harabi A., Harabi E., Chehalatt S., Zouai S., Karboua N.E. et Foughali L.: Effect of B_2O_3 on mechanical properties of porous natural hydroxyapatite derived from cortical bovine bones sintered at 1050°C. Des. Wat. Treat. 57(12), 5303-5309 (2016).

[11] Harabi E., Harabi A., Mezahi F.Z., Zouai S., Karboua N.E. et Chehalatt S.: Effect of P_2O_5 on mechanical properties of porous natural hydroxyapatite derived from cortical bovine bones sintered at 1050°C. Des. Wat. Treat. 57(12), 5297-5302 (2016).

[12] Harabi E., Harabi A., Foughali L., Chehlatt S., Zouai S. et Mezahi F.Z.: Grain growth in sintered natural hydroxyapatite. Acta Phy. Polonica A 127(4), 1161-1163 (2015).

[13] Harabi A. et Harabi E.: A modified milling system, using a bimodal distribution of highly resistant ceramics. Part1: A natural hydroxyapatite study. Mater. Sci. Eng. (C) 51, 206-215 (2015).

[14] Harabi A. et Chehlatt S.: Preparation process of a highly resistant wollastonite bioceramics using local raw materials. J. Therm. Anal. Calorim. 111, 203-211 (2013).

[15] Chehlatt S., Harabi A., Harabi E., Zouai S., Oudadesse H. et Barama S.E.: Biological properties study of bioactive wollastonite containing 5 wt% B_2O_3 prepared from local raw materials. Des. Wat. Treat. 57 (12), 5292-5296 (2016).

[16] Chehlatt S., Harabi A., Oudadesse H. et Harabi E.: In vitro bioactivity study of pure wollastonite prepared from local raw materials. Acta Phy. Polonica A 127(4), 925-927 (2015).

[17] Zouai S., Mezahi F., Achour S. et Harabi A.: A process for sintering of diopside prepared from dolomite. Mater. Sci. Forum 492-493, 235-240 (2005).

[18] Harabi A. et Zouai S.: A New and economic approach to synthesize and fabricate bioactive diopside ceramics using a modified domestic microwave oven. Part 1: Study of sintering and bioactivity. Int. J. Appl. Ceram. Technol. 11, 31-46 (2014).

[19] Kokubo T, Bioceramics and Their Clinical Applications. Kokubo T, Eds, Boca Raton, Florida: CRC Press, 2008.

[20] Hench L.L.: Biomaterials: a forecast for the future. Biomaterials 19, 1419-1423 (1998).

[21] De Aza P.N., De Aza A.H., Pena P. et De Aza S.: Bioactive glasses and glass ceramics. Bol. Soc. Esp. Ceram. 46, 45-55 (2007).

[22] Greenlee T.K.Jr., Beckham C.A., Crebo A.R. et Malmorg J.C.: Glass ceramic bone implants. J. Biomed. Mater. Res. 6(3), 235-244 (1972).

[23] Peitl O.: La Torre GP et Hench LL. Effect of crystallization on apatite layer formation on bioactive glass 45S5. J. Biomed. Mater. Res. 30(4), 509-514 (1996).

[24] Peitl O., Zanotto E.D. et Hench L.L.: Highly bioactive P_2O_5-Na_2O-CaO-SiO_2 glass-ceramics. J. Non-Cryst. Solids 292(1), 115-126 (2001).

[25] Li P., Yang Q., Zhang F. et Kokubo T.: The effect of residual glassy phase in a bioactive glass-ceramic on the formation of its surface apatite layer in vitro. J. Mater. Sci.: Mater. Med. 3, 452-456 (1992).

[26] Zanotto E.D., Ravagnani C., Peitl O., Panzeri H. et Lara E.H.G.: Process and compositions for preparing particulate, bioactive or resorbable biosilicates for use in the treatment of oral ailments, Patent WO/2004/074199, September 02 (2004).

[27] Siqueira R.L., Peitl O. et Zanotto E.D.: Gel-derived SiO_2–CaO–Na_2O–P_2O_5 bioactive powders: synthesis and in vitro bioactivity. Mater. Sci. Eng. C 31(5), 983-991 (2011).

[28] Lucas-Girot A., Mezahi F.Z., Mami M., Oudadesse H., Harabi A. et Le Floch M.: Sol–gel synthesis of a new composition of bioactive glass in the quaternary system SiO_2–CaO–Na_2O–P_2O_5: Comparison with melting method. J. Non-Cryst. Solids 57, 3322-3327 (2013).

[29] Mezahi F.Z/, Lucas-Girot A., Oudadesse H. et Harabi A.: Reactivity kinetics of 52S4 glass in the quaternary system SiO_2–CaO–Na_2O–P_2O_5: Influence of the synthesis process: Melting versus sol–gel. J. Non-Cryst. Solids 361, 111-118 (2013).
[30] Kokubo T., Kushitani H., Sakka S. et Yamamuro S.T.: Solutions able to reproduce in vivo surface- structure changes in bioactive glass-ceramic A–W. J. Biomed. Mater. Res. 24, 721-734 (1990).
[31] Martinez A., Izquierdo-Barba I. et Vallet-Regi M.: Bioactivity of CaO–SiO_2 binary glasses system. Chem. Mater. 12, 3080-3088 (2000).
[32] Sepulveda P., Jones J.R. et Hench L.L.: In vitro dissolution of melt derived 45S5 and sol-gel derived 58S bioactive glasses. J. Biomed. Mater. Res. 61, 301-311 (2002).
[33] ElBatal H.A., Azooz M.A., Khalil E.M.A., Soltan Monem A. et Hamdy Y.M.: Characterization of some bioglass–ceramics. Mater. Chem. Phys. 80, 599-609 (2003).
[34] Chang M.L. et Tanaka J.: FT-IR study for hydroxyapatite/collagen nanocomposite cross-linked by glutaraldehyde. Biomaterials 23, 4811-4818 (2002).

[35] Moura J., Teixeira L.N., Ravagnani C., Peitl O., Zanotto E.D., Beloti M.M., Panzeri H., Rosa A.L. et Oliveira P.T.: In vitro osteogenesis on a highly bioactive glass-ceramic (Biosilicate®). J. Biomed. Mater. Res. 82, 545-547 (2007).
[36] Aina V., Bertinetti L., Cerrato G., Cerruti M., Lusvardi G., Malavasi G., Morterra C., Tacconi L. et Menabue L.: On the dissolution/reaction of small-grain Bioglass® 45S5 and F-modified bioactive glasses in artificial saliva (AS). J. Appl. Surf. Sci. 257, 4185-4195 (2011).
[37] Vallet-Regi M., Romero A.M., Ragel C.V. et LeGeros RZ.: XRD, SEM-EDS, and FTIR studies of in vitro growth of an apatite-like layer on sol-gel glasses. J. Biomed. Mater. Res. 44(4), 416-421 (1999).
[38] Hench L.L.: Bioceramics-From Concept to Clinic. J. Am. Ceram. Soc. 74, 1487-1510 (1991).
[39] Kokubo T.: Novel Bioactive Materials. Anales de quimica Int. Ed. 93, 49-55 (1997).
[40] Ebisawa Y., Kokubo T., Ohura K. et Yamamuro T.: Bioactivity of Fe_2O_3 containing $CaOSiO_2$ glasses: in vitro evaluation. J. Mater. Sci: Mater. Med. 4, 225-232 (1992).
[41] Kokubo T, Yamamuro T et Hench LL, Handbook of Bioactive Ceramics. Vol. 1, Hench LL, Wilson J, Eds. Boca Raton, Florida: CRC Press, 1990: 41-49.
[42] Li P., Ohtsuki C., Kokubo T., Nakanishi K., Soga N., Nakamura T., Yamamuro T.: Process of Formation of Bone-Like Apatite Layer on Silica Gel. J. Mater. Sci: Mater. Med. 4, 127-13 (1993).
[43] Li P., Ye X., Kangasniem I., de Blieck-Hogervorst J.M.A., Klein C.P.A.T et Groot K.: In vivo calcium phosphate formation induced by sol-gel- prepared silica. J. Mater. Res. 29, 325-328 (1995).

[44] Kim C.Y., Clark A.E. et Hench L.L.: Compositional dependence of calcium-phosphate layer formation in fluoride bioglasses. J. Biomed. Mater. Res. 26, 1147-1161 (1992).
[45] Mami M., Lucas-Girot A., Oudadesse H., Dorbez-Sridi R., Mezahi F.Z. et Dietrich E.: Investigation of the surface reactivity of a sol–gel derived glass in the ternary system SiO2–CaO–P_2O_5. App. Sur. Sc. 254, 7386–7393 (2008).
[46] Iler RK. The Chemistry of Silica: Solubility, polymerization, colloid and surface properties and biochemistry. Wiley J & Sons, Eds. New York: Wiley Interscience, 1979: 453-462.
[47] Chen Q.Z., Thompson I.D., et Boccaccini A.R.: 45S5 Bioglass®-derived glass–ceramic scaffolds for bone tissue engineering. Biomaterials 27, 2414-2425 (2006).
[48] Boccaccini A.R., Chen Q., Lefebvre L., Gremillard L. et Chevalier J.: Sintering, crystallisation and biodegradation behaviour of Bioglass®-derived glass-ceramics. Faraday Discuss. 136, 27-44 (2007).
[49] Huang R., Pan J., Boccaccini A.R. et Chen Q.Z.: A two-scale model for simultaneous sintering and crystallization of glass-ceramic scaffolds for tissue engineering. Acta Biomater. 4, 1095-1103 (2008).
[50] Bretcanu O., Samaille C. et Boccaccini A.R.: Simple methods to fabricate Bioglass -derived glass-ceramic scaffolds exhibiting porosity gradient. J. Mater. Sci. 43, 4127-4134 (2008).